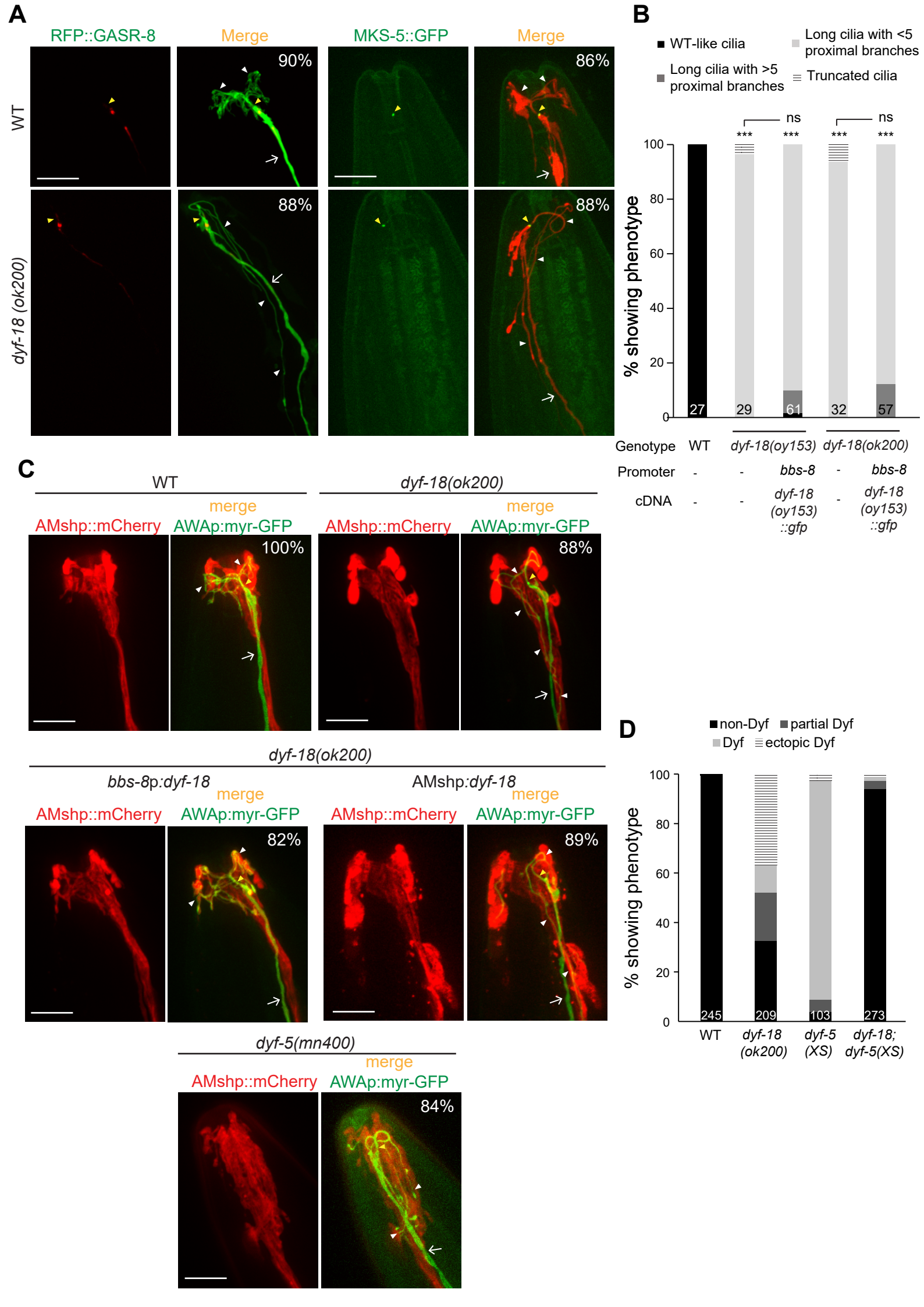
A
RFP::GASR-8
Merge
MKS-5::GFP
Merge
WT
dyf-18 (ok200)
90%
86%
88%
88%
B
WT-like cilia
Long cilia with <5 proximal branches
Long cilia with >5 proximal branches
Truncated cilia
ns
ns
***
***
***
***
% showing phenotype
100
80
60
40
20
0
27
29
61
32
57
Genotype
WT
dyf-18(oy153)
dyf-18(ok200)
Promoter
-
-
bbs-8
-
bbs-8
cDNA
-
-
dyf-18 (oy153) ::gfp
-
dyf-18 (oy153) ::gfp
C
WT
dyf-18(ok200)
AMshp::mCherry
merge
AWAp:myr-GFP
100%
88%
dyf-18(ok200)
bbs-8p:dyf-18
AMshp:dyf-18
82%
89%
dyf-5(mn400)
84%
D
non-Dyf
partial Dyf
Dyf
ectopic Dyf
% showing phenotype
100
80
60
40
20
0
245
209
103
273
WT
dyf-18 (ok200)
dyf-5 (XS)
dyf-18; dyf-5(XS)

Figure S1. DYF-18 acts neuronally to regulate AWA cilia morphology. Related to Figure 1 and Figure 2.

A) Representative images of AWA expressing the indicated fusion proteins in wild-type and *dyf-18(ok200)* animals. Cilia were visualized via expression of *gpa-4Δ6*p*::myr-gfp* or *gpa-4Δ6*p*::mCherry*. Numbers at top right indicate the percentage of neurons exhibiting the shown phenotypes; n≥30 neurons each in 3 independent experiments. The cilia base and cilia are indicated by yellow and white arrowheads, respectively; the dendrite is marked by an arrow. Anterior is at top in all images. Scale bars: 10 μm.

B) Percentage of adult hermaphrodites of the indicated genotypes exhibiting AWA cilia phenotypes. Numbers in each bar indicate the number of examined neurons in 2-3 independent experiments. *** indicates different from wild-type at $P<0.001$; ns – not significant (Wilcoxon rank-sum test).

C) Representative images of AWA (green) and the amphid sheath cell (red) in adult hermaphrodites of the indicated genotypes. AWA was visualized via expression of *gpa-4Δ6*p*::myr-gfp*, the amphid sheath cell was visualized via expression of *F16F9.3*p*::mCherry* (gift of Shai Shaham) [S1]. Wild-type *dyf-18* sequences were expressed in ciliated neurons or the amphid sheath cell under the *bbs-8* and *F16F9.3* promoters, respectively. Numbers at top right indicate the percentage of neurons exhibiting the shown phenotypes; n≥30 neurons each in 3 independent experiments. The cilia base and cilia are indicated by yellow and white arrowheads, respectively; the dendrite is marked by an arrow. Anterior is at top in all images. Scale bars: 10 μm.

D) Percentages of neurons in adult hermaphrodites of the indicated genotypes exhibiting dye-filling phenotypes. Numbers in each bar indicate the number of examined animals in

2 independent experiments. Non-Dyf – dye uptake in 12 pairs of amphid sensory neurons; partial Dyf – dye uptake in <12 pairs of amphid sensory neurons; Dyf – no dye uptake in amphid sensory neurons; ectopic Dyf – dye uptake in additional sensory neurons.

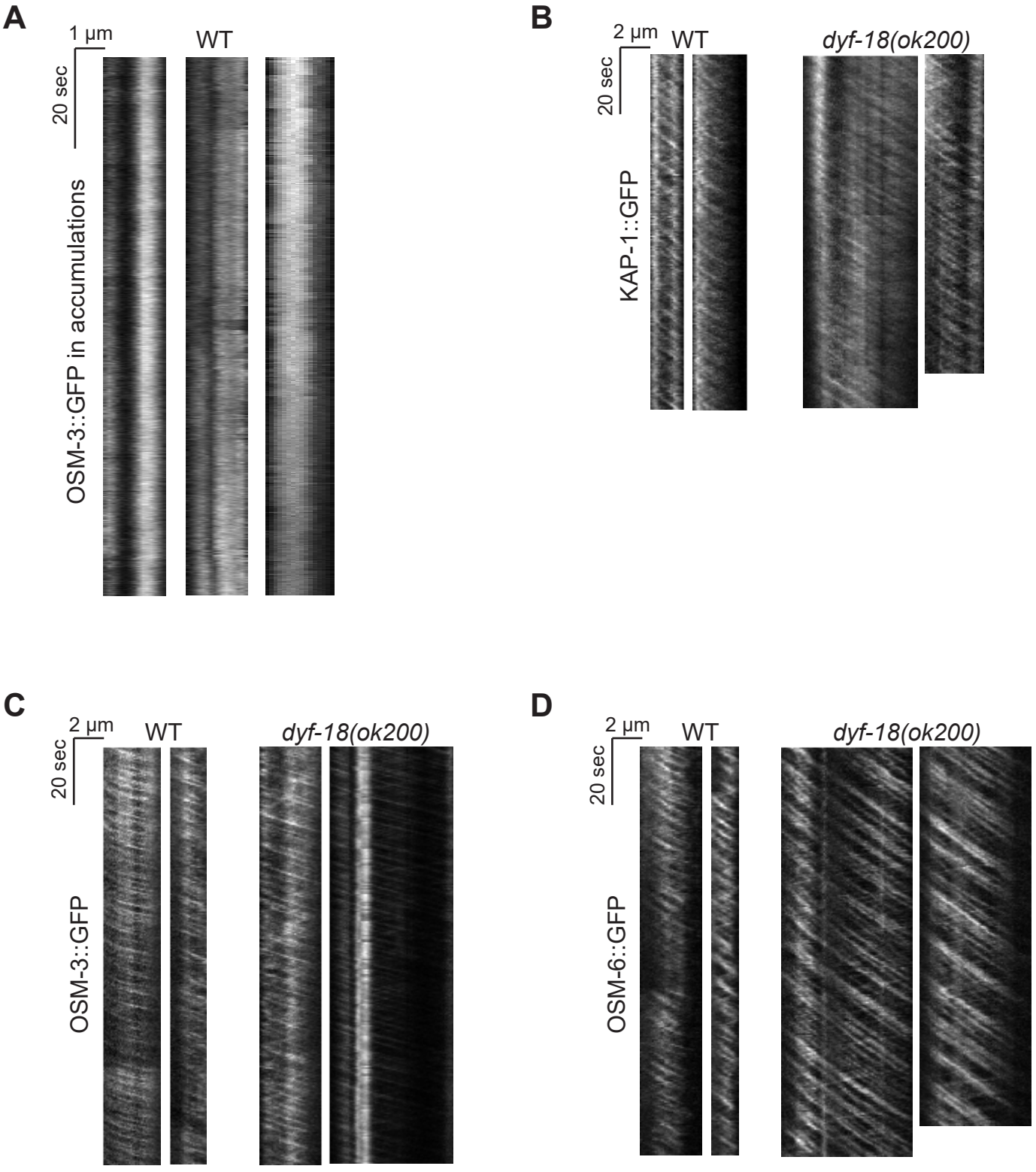
A
1 µm
20 sec
WT
OSM-3::GFP in accumulations
B
2 µm
20 sec
WT
dyf-18(ok200)
KAP-1::GFP
C
2 µm
20 sec
WT
dyf-18(ok200)
OSM-3::GFP
D
2 µm
20 sec
WT
dyf-18(ok200)
OSM-6::GFP

Figure S2. Localization and movement of IFT motors in AWA cilia. Related to Figure 4.

A) Representative kymographs of immobile OSM-3::GFP at the distal tips of wild-type AWA cilia. Three independent examples are shown.

B-D) Representative kymographs of KAP-1:GFP (B), OSM-3::GFP (C) and OSM-6::GFP (D) movement in the proximal stalks of AWA cilia in wild-type and *dyf-18(ok200)* mutants. Two independent examples are shown for each.

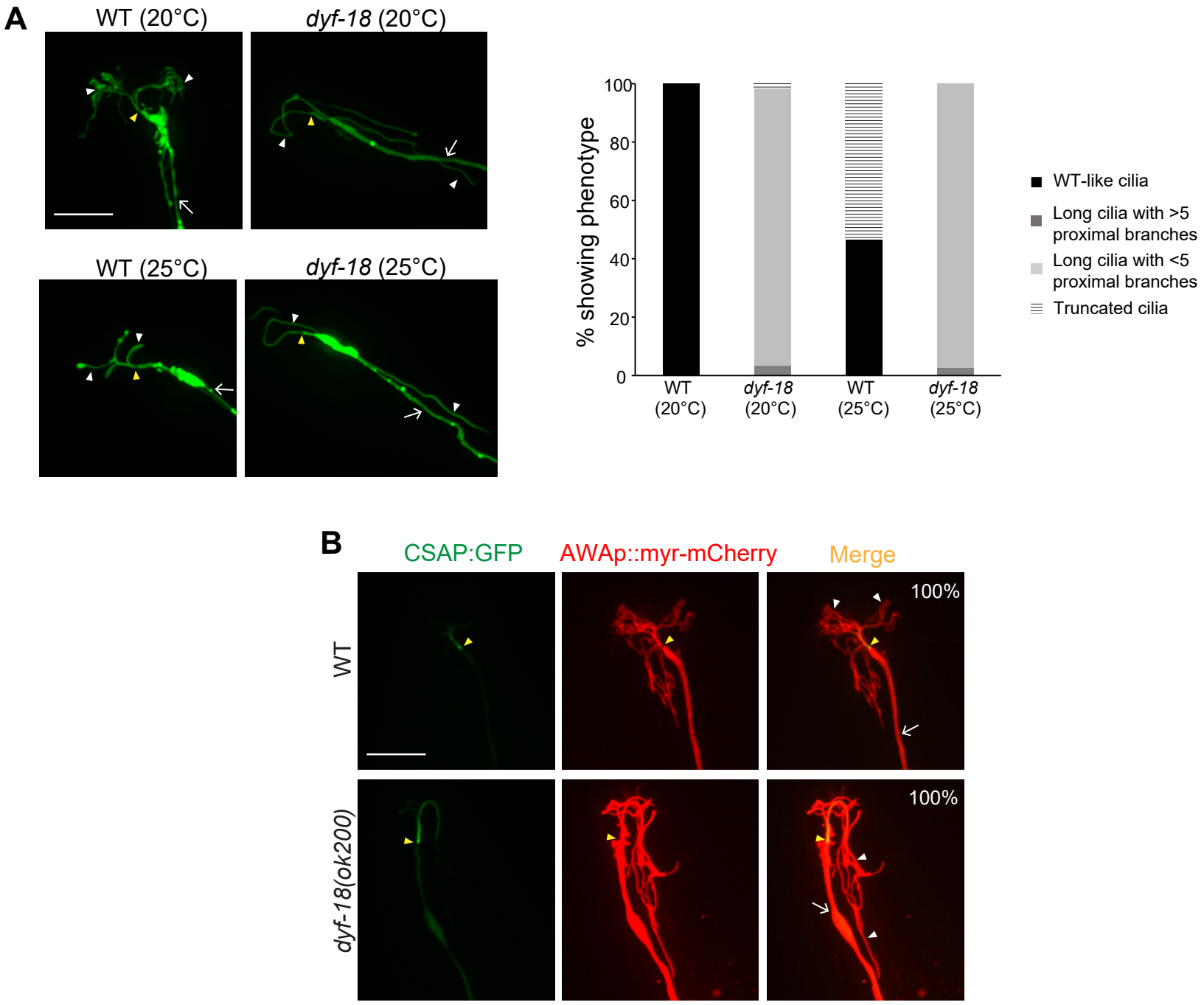
A
WT (20°C)
dyf-18 (20°C)
WT (25°C)
dyf-18 (25°C)
% showing phenotype
100
80
60
40
20
0
WT (20°C)
dyf-18 (20°C)
WT (25°C)
dyf-18 (25°C)
WT-like cilia
Long cilia with >5 proximal branches
Long cilia with <5 proximal branches
Truncated cilia
B
CSAP:GFP
AWAp::myr-mCherry
Merge
WT
dyf-18(ok200)
100%
100%

Figure S3. AWA axonemal stability is altered in *dyf-18* mutants. Related to Figure 5 and Figure 6.

A) Representative images (left) and quantification of AWA cilia morphologies (right) in wild-type and *dyf-18(ok200)* mutant animals grown at 20°C and 25°C. The cilia base and cilia are indicated by yellow and white arrowheads, respectively; the dendrite is marked by an arrow in images at left. n≥30 neurons. Anterior is at left. Scale bar: 10 μm.

B) Representative images of the localization of the polyglutamylated tubulin binding protein CSAP [S2] in wild-type and *dyf-18(ok200)* mutants. The cilia base and cilia are indicated by yellow and white arrowheads, respectively; the dendrite is marked by an arrow. Numbers at top right indicate the percentage of neurons exhibiting the shown phenotypes; n≥30 in 3 independent experiments. Scale bar: 10 μm.

A

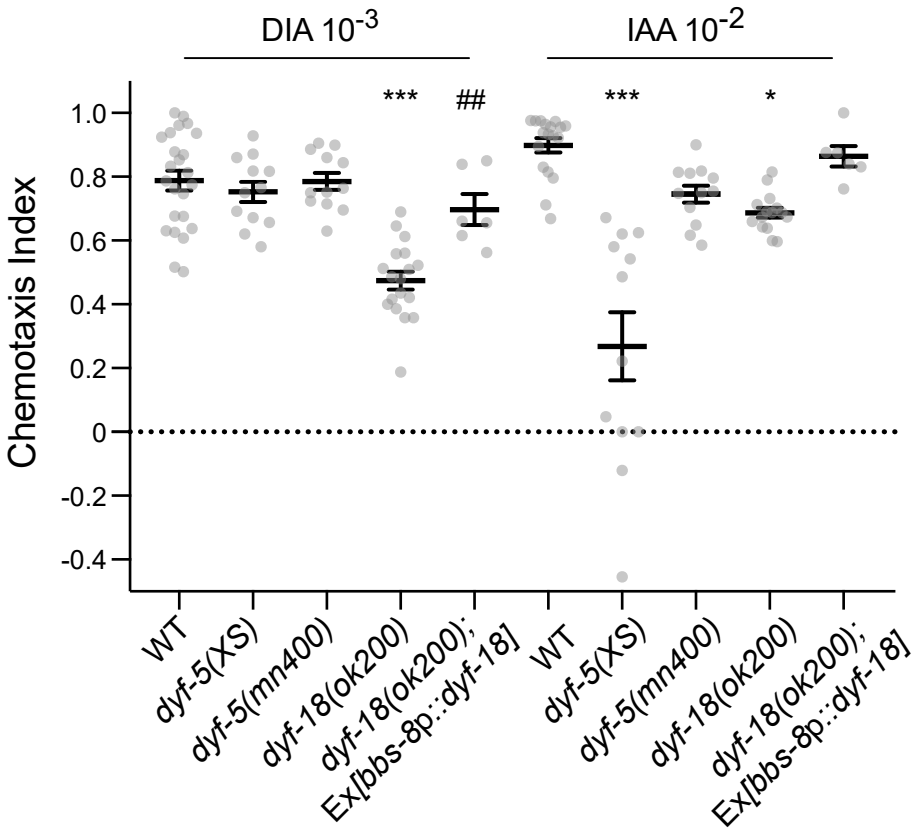
DIA 10-3
IAA 10-2
Chemotaxis Index
1.0
0.8
0.6
0.4
0.2
0
-0.2
-0.4
***
##
***
*
WT
dyf-5(XS)
dyf-5(mn400)
dyf-18(ok200)
dyf-18(ok200); Ex[bbs-8p::dyf-18]
WT
dyf-5(XS)
dyf-5(mn400)
dyf-18(ok200)
dyf-18(ok200); Ex[bbs-8p::dyf-18]

B

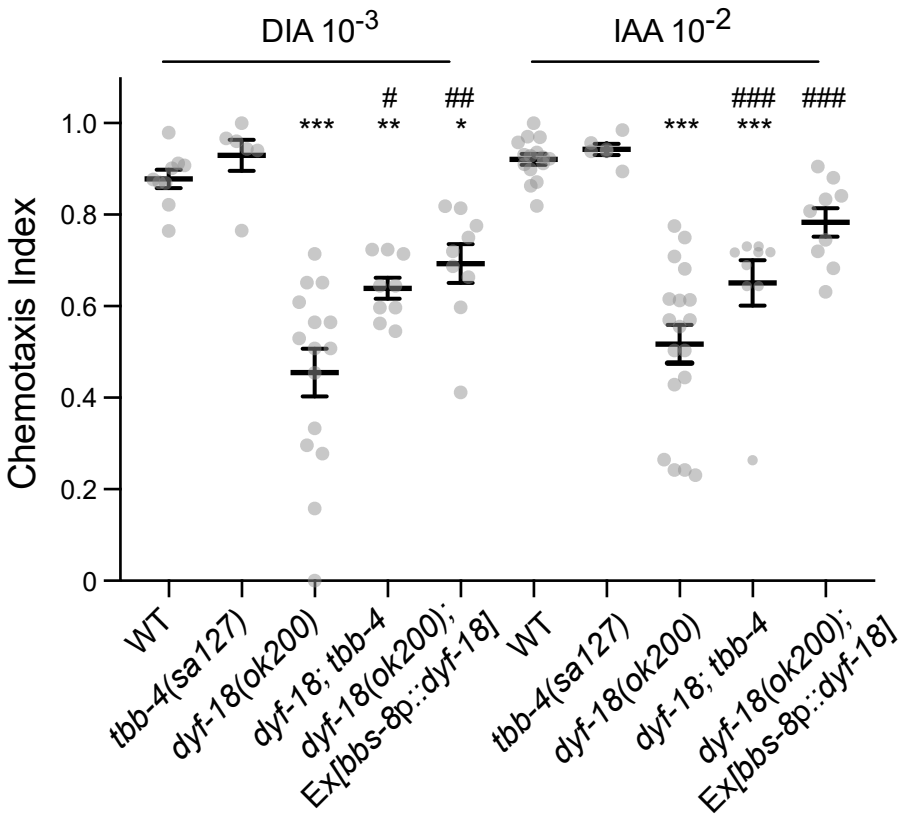
DIA 10-3
IAA 10-2
Chemotaxis Index
1.0
0.8
0.6
0.4
0.2
0
***
#
**
##
*
***
###
***
###
WT
tbb-4(sa127)
dyf-18(ok200)
dyf-18; tbb-4
dyf-18(ok200); Ex[bbs-8p::dyf-18]
WT
tbb-4(sa127)
dyf-18(ok200)
dyf-18; tbb-4
dyf-18(ok200); Ex[bbs-8p::dyf-18]

Figure S4. Sensory behavioral phenotypes of *dyf-5* and *dyf-18* mutants. Related to Figure 6.

A, B) Behavioral responses of adult animals of the indicated genotypes to a point source of diacetyl (DIA) diluted to 10^{-3} and isoamyl alcohol (IAA) diluted to 10^{-2}. Chemotaxis index = (number of animals in plate segments containing the odor) – (number of animals in plate segments containing ethanol)/total number of animals. Horizontal bar indicates mean, errors are SEM. Each dot is the chemotaxis index of a single assay with ~100 animals; assays were performed at least in triplicate on three independent days. *, **, and *** indicate different from wild-type at $P<0.05$, 0.01, and 0.001, respectively; #, ## and ### indicate different from *dyf-18(ok200)* at $P<0.05$, 0.01 and 0.001, respectively (ANOVA with Tukey's posthoc corrections). Animals in A and B were grown at 20°C and 15°C, respectively.

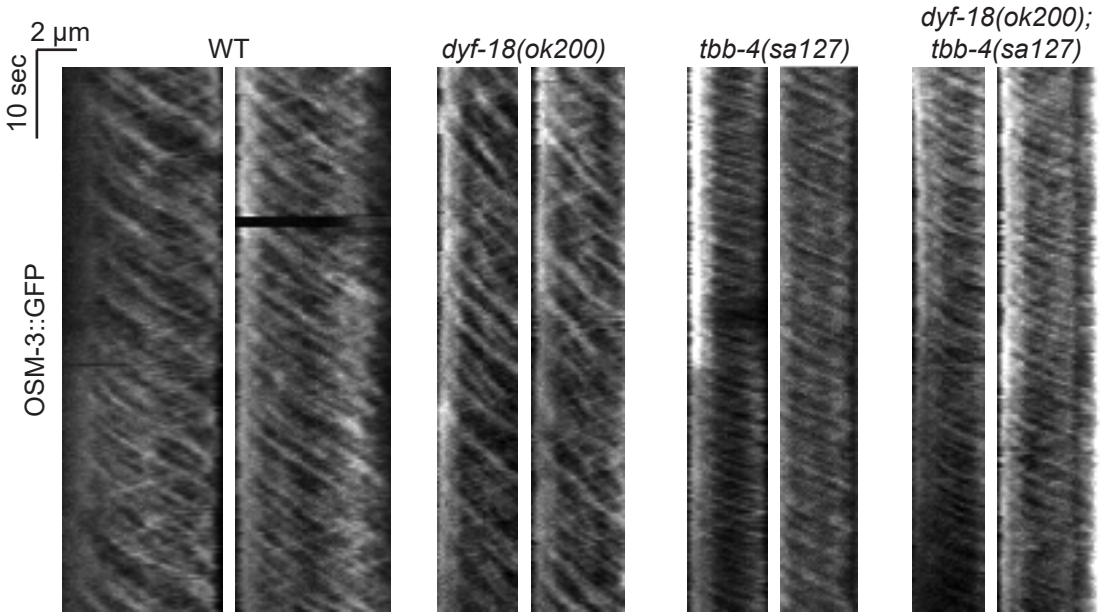
2 µm
10 sec
OSM-3::GFP
WT
dyf-18(ok200)
tbb-4(sa127)
dyf-18(ok200);
tbb-4(sa127)

Figure S5. Movement of OSM-3::GFP in ASH cilia. Related to Figure 7.

Shown are two representative kymographs each for OSM-3::GFP movement in the ASH cilia of animals of the indicated genotypes. Velocities shown in Table S3 were calculated from the first halves of the kymographs in wild-type, *dyf-18* and *dyf-18; tbb-4* double mutants (middle segments).

Table S1. Anterograde IFT velocities in AWA cilia. Related to Figure 4.

Strain	Fusion protein[a]	Mean anterograde velocity (μm/sec ± SD)[b]	n/N
Wild-type	KAP-1::GFP	0.66 ± 0.15	322/16
dyf-18(ok200)	KAP-1::GFP	0.70 ± 0.12	609/27
Wild-type	OSM-3::GFP	1.34 ± 0.43	742/17
dyf-18(ok200)	OSM-3::GFP	1.30 ± 0.37	425/16
Wild-type	OSM-6::GFP	0.72 ± 0.25	701/27
dyf-18(ok200)	OSM-6::GFP	0.90 ± 0.52[c]	745/15

[a]All fusion proteins were expressed under the *gpa-4Δ6* promoter.

[b]IFT was quantified in the proximal stalk of wild-type cilia, and in a region approximately 7 μm from the cilia base in *dyf-18* mutants.

[c]Different from wild-type at $P<0.001$.

All analyses were performed in one day old adult hermaphrodites grown at 20°C. n: number of GFP particles; N: number of cilia.

Also see Figure S2B-D.

Table S2. AWA cilia morphology in animals mutant for tubulin post-translational modification genes. Related to Figure 6.

Genotype	Percentage of neurons exhibiting phenotype:			n	References
	Wild-type	Elongated	Truncated		
atat-2(ok2415)	92.6	0.0	7.4	27	[S3]
dyf-18(ok200); atat-2(ok2415)	0.0	89.7	10.3	29	
ccpp-1(ok1821)	89.7	0.0	10.3	29	[S4]
ccpp-1(ok1821); dyf-18(ok200)	7.4	85.2	7.4	27	
klp-13(oy154)	96.2	0.0	3.8	26	[S5]
dyf-18(ok200); klp-13(oy154)	0.0	95.2	4.8	21	
ccpp-6(ok382)	91.3	0.0	8.7	23	[S6]
ccpp-6(ok382); dyf-18(ok200)	5.7	88.6	5.7	35	
ttll-4(tm3310)	95.7	0.0	4.3	23	[S4, S6]
ttll-4(tm3310); dyf-18(ok200)	4.0	92.0	4.0	25	
mec-17(ok2109)	96.7	0.0	3.3	30	[S7]

Table S3. Anterograde OSM-3::GFP velocities in the middle segments of ASH cilia. Related to Figure 7.

Strain expressing OSM-3::GFP[a]	Mean anterograde velocity (μm/sec ± SD)[b]	n/N
Wild-type	0.63 ± 0.18	866/31
dyf-18(ok200)	0.46 ± 0.15[c]	670/43
tbb-4(sa127)	0.95 ± 0.29[c]	811/40
dyf-18(ok200); tbb-4(sa127)	0.75 ± 0.28[d,e]	864/41

[a]OSM-3::GFP was expressed under the *sra-6* promoter.
[b]IFT velocities were quantified in the middle segments of ASH cilia.
[c]Different from wild-type at $P<0.001$.
[d]Different from *dyf-18* at $P<0.001$.
[e]Different from *tbb-4* at $P<0.001$.
All analyses were performed in one day old adult hermaphrodites grown at 15°C. n: number of GFP particles; N: number of cilia.
Also see Figure S5.

Supplemental References

S1. Bacaj, T., Tevlin, M., Lu, Y., and Shaham, S. (2008). Glia are essential for sensory organ function in *C. elegans*. Science *322*, 744-747.

S2. Backer, C.B., Gutzman, J.H., Pearson, C.G., and Cheeseman, I.M. (2012). CSAP localizes to polyglutamylated microtubules and promotes proper cilia function and zebrafish development. Mol Biol Cell *23*, 2122-2130.

S3. Shida, T., Cueva, J.G., Xu, Z., Goodman, M.B., and Nachury, M.V. (2010). The major alpha-tubulin K40 acetyltransferase alphaTAT1 promotes rapid ciliogenesis and efficient mechanosensation. Proc Natl Acad Sci USA *107*, 21517-21522.

S4. O'Hagan, R., Piasecki, B.P., Silva, M., Phirke, P., Nguyen, K.C., Hall, D.H., Swoboda, P., and Barr, M.M. (2011). The tubulin deglutamylase CCPP-1 regulates the function and stability of sensory cilia in *C. elegans*. Curr Biol *21*, 1685-1694.

S5. Niwa, S., Nakajima, K., Miki, H., Minato, Y., Wang, D., and Hirokawa, N. (2012). KIF19A is a microtubule-depolymerizing kinesin for ciliary length control. Dev Cell *23*, 1167-1175.

S6. Kimura, Y., Kurabe, N., Ikegami, K., Tsutsumi, K., Konishi, Y., Kaplan, O.I., Kunitomo, H., Iino, Y., Blacque, O.E., and Setou, M. (2010). Identification of tubulin deglutamylase among *Caenorhabditis elegans* and mammalian cytosolic carboxypeptidases (CCPs). J Biol Chem *285*, 22936-22941.

S7. Akella, J.S., Wloga, D., Kim, J., Starostina, N.G., Lyons-Abbott, S., Morrissette, N.S., Dougan, S.T., Kipreos, E.T., and Gaertig, J. (2010). MEC-17 is an alpha-tubulin acetyltransferase. Nature *467*, 218-222.